



## Rainwater chemical evolution driven by extreme rainfall in megacity: Implication for the urban air pollution source identification

Jie Zeng, Guilin Han\*, Shitong Zhang, Xuhuan Xiao, Yikai Li, Xi Gao, Di Wang, Rui Qu

Institute of Earth Sciences, China University of Geosciences (Beijing), Beijing, 100083, China



### ARTICLE INFO

Handling Editor: M.T. Moreira

**Keywords:**

Extreme precipitation  
Rainwater chemistry  
Rain scouring  
Neutralization  
Source identification  
Beijing

### ABSTRACT

Atmospheric pollution has become a global environmental issue, which caused a number of human health threats. It is therefore vital to understand the source-sink processes of air pollutants and their mechanisms. Rainwater is not only the major sink (removal process) of air pollutants, but also the good source tracer of atmospheric components. On the background of global climate changes, the extreme rainfall exerts a serious influence in megacity. However, the extreme rainfall driven chemical evolution of rainwater and its reflection on air pollution are rarely focused, even though it plays a significant role in urban-surficial ecosystem. To better understand the chemical evolution of urban extreme rainfall and their potential environmental effects, rainwater samples were collected in Beijing, a typical megacity, during the extreme rainfall period in 2021. Based on rainwater stoichiometry and historical comparison, the scouring process of air substance, the neutralizing process of rainwater and the ion sources were revealed. The findings showed that  $\text{NH}_4^+$ ,  $\text{NO}_3^-$ ,  $\text{SO}_4^{2-}$ , and  $\text{Ca}^{2+}$  were four primary rainwater ions with distinct daily variations which were well removed by rainwater scouring process. The high values of NF (neutralization factor, ~2.2) and NP/AP (ratio of neutralizing to acidifying potential, ~1.8) suggested a relatively high level of rainwater neutralization. Source identification revealed that rainwater  $\text{SO}_4^{2-}$  (94.9%) and  $\text{NO}_3^-$  (99.9%) were primarily originated from anthropogenic input, particularly the mobile emission sources (transportation), while sea salt input represented the major  $\text{Cl}^-$  source (86.9%) and all  $\text{Na}^+$  source. By contrast, crust dust input was the main contributor of rainwater  $\text{K}^+$  (94.0%),  $\text{Mg}^{2+}$  (92.3%) and  $\text{Ca}^{2+}$  (98.2%), whereas  $\text{NH}_4^+$  was considered only the contribution of human input (e.g., municipal feces and fossil fuel burning). This study clarified the chemical characteristics of extreme rainfall in megacity and highlighted the significant impact on urban environment, which will benefit the urban environmental management in the context of global climate change.

### 1. Introduction

With the continuous growth of the world population, and the acceleration of global urbanization, the increase air pollutants emission was widely found in the urban region, especially megacities, which caused the different air pollution problems and potential human exposure to health risks, such as respiratory and cardiovascular diseases (Jaspreeet and Charu, 2021). As an important removal mechanism/process of air pollutants, rainfall was considered as an effective indicator of source of atmospheric components, and has received widely attention in the academic communities (Keresztesi et al., 2019). Moreover, the extreme rainfall (or rainstorm) events in urban areas and megacities have been frequently occurred in various countries in the world (Arnbjerg-Nielsen et al., 2013), including China (Zhou et al.,

2017). For example, a rainstorm in July 2012 formed a total rainfall amount of 535 mm, breaking the China's highest record in the past 60 years (Li et al., 2019). A maximum precipitation of 460 mm in 24 h was recorded on July 21, 2012 in Beijing area, causing by the combined action of Bengal Bay-derived southwestern monsoonal moisture and typhoon-caused southeastern moisture transport (Li et al., 2021). Previous studies showed that the anomalous small and medium-scale circulations jointly affected the short-term extreme rainfall in Beijing (Yang et al., 2021a). Moreover, the high degree of urbanization is also an important driving factor of rainfall events under the background of warming climate (Yang et al., 2021b). In the flood season of 2021, extreme heavy rainfall events occurred in North China (Zhong et al., 2021), and some cities in North China received the highest rainfall amount levels ever recorded (Zhang et al., 2021a). Obviously, Beijing is

\* Corresponding author.

E-mail address: [hanguilin@cugb.edu.cn](mailto:hanguilin@cugb.edu.cn) (G. Han).

also one of the cities in North China hit by extreme rainfall in the flood season of 2021.

Extreme rainfall event is one of the most common natural disasters under the background of global climate changes, which induced landslides/debris flow in mountain areas and inland inundation in urban region, which further hazard human society and environment due to their destructive power (Li et al., 2019). The extreme rainstorm-related studies generally focus on the major risks of inundated area after long distance movement of rainfall-driven runoff (Yang et al., 2019), and the impacts on urban drainage systems (Arnbjerg-Nielsen et al., 2013). However, the evolution of chemical composition, material provenance, and potential risks of rainwater itself during the extreme rainstorm are relatively less reported. In fact, rainfall is the most important sink process of atmospheric matters, in particular, the air pollutants (Keresztesi et al., 2020). Rainwater chemistry is generally changed by the in- and below-cloud rainfall processes with atmospheric matters scouring (Ge et al., 2021). Thus, rainwater chemical compositions can reflect the atmospheric environmental information (air quality), indicate the sources of major rainwater chemicals (Zeng et al., 2020a), and further influence/drive the hydrochemistry of earth-surface hydrosphere (Qin et al., 2020), such as rivers, lakes/reservoirs (Wu and Han, 2018), and streams (Wang et al., 2022).

Beijing, the capital of China, is one of largest megacities over the world with tens of millions of people and high levels of urbanization, facing serious air pollution and precipitation acidification (Sun et al.,

2021). As a significant part of “Joint prevention and control of atmospheric pollution” in the Jingjinji (Beijing, Tianjin, and Hebei) region, previous studies have already investigated the rainwater chemistry and wet deposition from different perspectives, including the below-cloud scavenging process (Ge et al., 2021), acidification characteristics (Sun et al., 2021), and the strontium isotope tracing (Xu et al., 2012). Moreover, previous work revealed that the atmospheric aerosol can modify the distribution of rainfall center via the direct and indirect effect, and the concentrate rainfall occurred in urban regions during the extreme rainfall event in Beijing (Zhang et al., 2021b), which could further impact the rainwater chemistry. However, the chemical evolution of extreme rainfall-driven rainwater is rarely reported.

In this study, we collected the rainwater samples in Beijing urbanized area (Haidian District) during the extreme rainstorm period from July to August in 2021. The daily-based rainwater sampling is implemented to collect samples. Rainwater samples were obtained for chemical analysis of major ions. Together with the air pollutant concentration data and the historical rainwater chemical data, the rainwater chemical evolution driven by extreme rainfall in such a megacity is reflected. The main objectives of this work includes (1): exploring the rainwater chemical compositions and the daily-scale variations during extreme rainfall period, (2) clarifying the rainwater scouring processes of rainwater chemistry, (3) evaluating the neutralization capacity of rainwater, (4) identifying the potential sources of rainwater chemicals and their environmental effects.

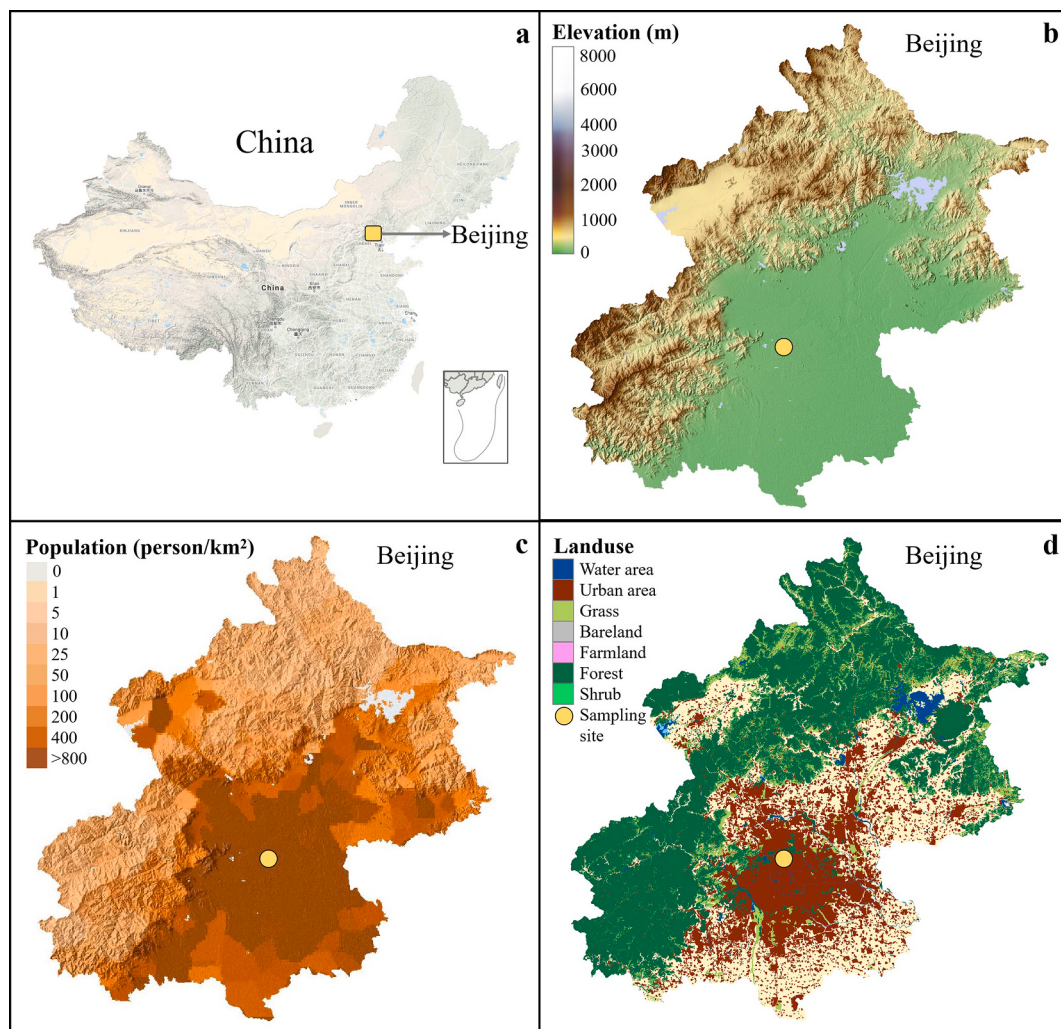


**Fig. 1.** The rainwater sampling site in Beijing: (a) the location of Beijing in China; (b) the elevation distribution; (c) the population density; (d) the land use distribution.

## 2. Methodology

### 2.1. Study area

Beijing is located at the north region of the North China Plain, approximately 150 km to the Sea (Fig. 1a). This city is surrounded by mountains from three sides (west, north and northeast) with the higher terrain in northwest mountain region and the lower terrain in southeast plain area (Fig. 1b). The altitude of this city is between 20 and 2303 m. The lithology distribution of Beijing is primarily dolomite, shale, limestone, marble conglomerate and various fluvial deposits (Li et al., 2019). This city is characterized by a semi-arid climatic zone, a representative continental monsoon climate and four distinct seasons (Xu and Han, 2009), where the yearly average rainfall amount ranged between 400 and 800 mm (Li et al., 2019), the monthly average air temperature from  $-3$  to  $28$  °C, and the monthly average humidity from 38% to 68%. Generally, three quarters of the total annual rainfall occurred in July and August in the form of thunderstorms (Li et al., 2019).

Beijing is a crowded city with extremely high population density and car ownership. According to the Beijing Municipal Bureau of Statistics, by the end of 2020, the number of civil motor vehicles has reached 6.57 million, and the permanent population has reached 21.89 million, with an average population density of 1334 people/km<sup>2</sup> (even up to 6602–21888 people/km<sup>2</sup> in the central urban area) (Fig. 1c). The large population is concentrated in central Beijing, resulting in the higher degree of urbanization and obvious differences in land cover between urban and suburban areas (Fig. 1d). Since the 1980s, Beijing has undergone fast economic development and transportation expansion, causing serious atmospheric contamination (Xu et al., 2012). The significant rainwater acidification has been observed in the past twenty years, especially during 2001–2016 with the acid rain frequency of 10%–38.6% (Fig. 2a). The highest acid-rain frequency and lowest annual average rainwater pH value ( $\sim 4.8$ ) was observed in 2008 (Fig. 2a). Meanwhile, the annual rainfall amount in Beijing has basically presented a fluctuating rising trend since the beginning of the 21st century (Fig. 2b) (Sun et al., 2021). With the promotion of atmospheric pollution control, the atmospheric NO<sub>2</sub> concentrations have declined with the total descending percentage of  $\sim 52\%$  in the past twenty years (rebounding slightly from 2008 to 2014), while the substantial decline of total SO<sub>2</sub> was observed (Fig. 2c). These results further lead to the

increasing ratio of atmospheric NO<sub>2</sub> and SO<sub>2</sub> concentrations (Fig. 2c).

### 2.2. Sample collection and measurement

The sampling site was set at the typical urban area of Beijing City (Haidian District, 39.99°N, 116.35°E, Fig. 1). The rainwater samples were collected via a polyethylene (PE) sampler placed in an open area without any external influences (e.g., trees and buildings). The lid of PE sampler was covered on non-rainy time to avoid dust deposition. The sampler was cleaned by ultrapure water and air-dried before each sampling process. The rainwater samples were collected manually and divided in a daily-scale. A total of 20 rainwater samples were obtained during July to August 2021. The cumulative rainfall amount in July and August were 355.9 and 186.1 mm, respectively, significantly higher than the multi-year average value of the corresponding months (Fig. S1a). The pH and electrical conductivity (EC) were detected by the multi-parameter meter. After the filtrate processes by the acetate membrane filters (0.22 µm), all samples were refrigerated at 0–4 °C and finally measured at the Institute of Geographic Sciences and Natural Resources Research, Chinese Academy of Sciences, following the detection procedures of our previous work (Zeng et al., 2020a). In brief, the rainwater anions (F<sup>-</sup>, Cl<sup>-</sup>, SO<sub>4</sub><sup>2-</sup>, and NO<sub>3</sub><sup>-</sup>) were measured by ionic chromatography (IC, Dionex 1100) and the cations (Na<sup>+</sup>, K<sup>+</sup>, Mg<sup>2+</sup>, and Ca<sup>2+</sup>) were detected by Inductively Coupled Plasma Optical Emission Spectrometer (ICP-OES, Optima 5300DV). The NH<sub>4</sub><sup>+</sup> was determined by the spectrophotometer with Nessler method. The sample replicates and procedural blanks were applied to ensure the measurement quality. The relative standard deviation of repeated measurements is within  $\pm 5\%$ . The quality control was also conducted via the ionic balance (Fig. S1b) and presented a good quality of chemical detection, which was similar to previous studies of Beijing rainwater (Xu et al., 2015). Moreover, the meteorological parameter data, including precipitation amount, air temperature, and humidity during the sampling period were taken from the Weather China (<http://www.weather.com.cn/>). The air pollutant concentration data (SO<sub>2</sub>, NO<sub>2</sub>, PM<sub>2.5</sub>, and PM<sub>10</sub>) were collected from the Haidian Wanliu monitoring station reported by Beijing Municipal Ecological Environmental Monitoring Center.

### 2.3. Calculation processes

The volume-weighted mean (VWM) concentrations of rainwater ions during the whole study period are calculated as follow (Zeng et al., 2020d):

$$C = \frac{\sum C_i P_i}{\sum P_i} \quad (1)$$

where C, C<sub>i</sub>, P<sub>i</sub>, are the VWM concentration (µeq L<sup>-1</sup>), concentration of daily sample (µeq L<sup>-1</sup>), and daily rainfall amount.

The fractional acidity (FA) is calculated to evaluate the neutralization degree by the rainwater alkaline components as follow (Wu et al., 2012):

$$FA = \frac{c(H^+)}{c(SO_4^{2-}) + c(NO_3^-)} \quad (2)$$

where the c(H<sup>+</sup>), c(SO<sub>4</sub><sup>2-</sup>), and c(NO<sub>3</sub><sup>-</sup>) are the corresponding ion concentrations (µeq L<sup>-1</sup>). The c(H<sup>+</sup>) is converted by pH value. Rainwater acidity is barely neutralized when FA = .

The specific contribution of each alkaline ions on rainwater neutralization are assessed by the neutralization factors (NF) (Wu and Han, 2015):

$$NF_{Xi} = \frac{c(X_i)}{c(SO_4^{2-}) + c(NO_3^-)} \quad (3)$$

where c(X<sub>i</sub>) is the concentrations of alkaline ions, including Ca<sup>2+</sup>, NH<sub>4</sub><sup>+</sup>,

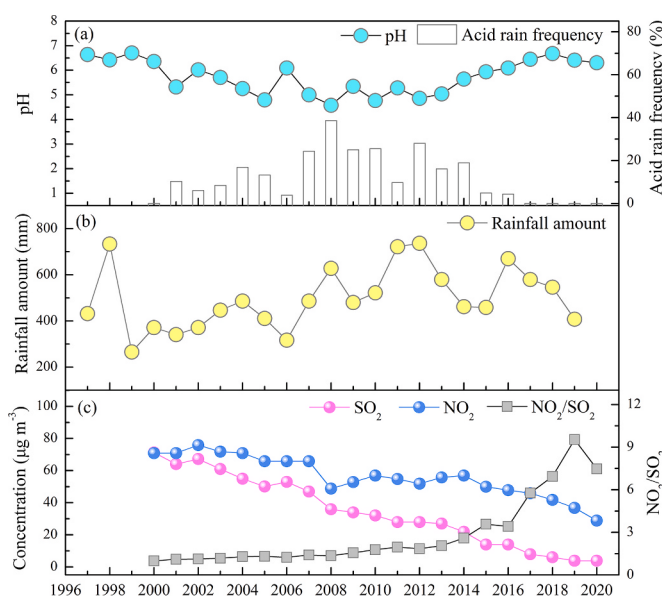


Fig. 2. Historical changes of (a) annual pH values and acid rain frequency; (b) rainfall amount; (c) NO<sub>2</sub> and SO<sub>2</sub> concentrations, and ratios. Data are from (Sun et al., 2021).

$\text{Na}^+$ ,  $\text{K}^+$ ,  $\text{Mg}^{2+}$  ( $\mu\text{eq L}^{-1}$ ).

The neutralizing potential (NP) and acidifying potential (AP) ratios are also evaluated as follow (Zeng et al., 2020c):

$$NP / AP = \frac{c(\text{Ca}^{2+}) + c(\text{NH}_4^+)}{c(\text{SO}_4^{2-}) + c(\text{NO}_3^-)} \quad (4)$$

where  $c(\text{Ca}^{2+})$ ,  $c(\text{NH}_4^+)$ ,  $c(\text{SO}_4^{2-})$ , and  $c(\text{NO}_3^-)$  are the corresponding ion concentrations ( $\mu\text{eq L}^{-1}$ ).

### 3. Results and discussion

#### 3.1. Rainwater ion compositions during extreme rainfall period

##### 3.1.1. Ion compositions

The statistical results of major rainwater ion concentrations and the water parameters (pH, EC) during the study period (together with the reported data from 1995 to 2018) are listed in Table 1. The rainwater EC values ranged from 15 to 157  $\mu\text{S cm}^{-1}$  with a VWM value of 47  $\mu\text{S cm}^{-1}$ , while the rainwater pH values varied between 6.5 and 7.5 with a VWM value of 6.9. The total anion concentration was slightly lower than the total cation concentration (Fig. S1b), indicating well detection of most rainwater components (ions) (Han et al., 2019). The contribution of some organic anionic species (e.g., vegetation-derived oxalate) can be the interpretation of slightly lower concentration of total anions (Zhang et al., 2011). There existed large variations of each ion concentration, and significantly higher mean values of most ion concentrations (relative to median values, Table 1). Therefore, the VWM concentrations of each ion were used for comparison. The VWM concentrations of rainwater ions in this study were in the ordered of  $\text{NH}_4^+ > \text{NO}_3^- > \text{SO}_4^{2-} > \text{Ca}^{2+} > \text{Mg}^{2+} > \text{Cl}^- > \text{Na}^+ > \text{K}^+ > \text{F}^-$ . Compared with the reported data of rainwater ion compositions from 1995 to 2018 (Table 1), the rainwater EC in this work was close to the adjacent 2017 and 2018, but lower than that in 2006–2012. The  $\text{F}^-$  concentration was always maintained at a low level, and the lowest  $\text{F}^-$  concentration was still found in 2021 (extreme rainfall period). The concentrations of  $\text{Cl}^-$ ,  $\text{Na}^+$ , and  $\text{K}^+$  were also relatively lower compared with previous years, whereas the  $\text{Mg}^{2+}$  concentration was close to that of 2017. Notably, the concentrations of representative anthropogenic-derived ions ( $\text{NO}_3^-$  and  $\text{SO}_4^{2-}$ ) in this work were significantly declined compared to the high-frequency acid rain years before 2012, while the rainwater  $\text{NH}_4^+$  invariably presented a high concentration level since 1995.

The percentages of each ion in rainwater are shown in Fig. 3, which obviously indicated that the primary rainwater ions are  $\text{NO}_3^-$ ,  $\text{SO}_4^{2-}$ ,  $\text{NH}_4^+$ , and  $\text{Ca}^{2+}$ .  $\text{NO}_3^-$  was the most enrich anion (47.1% of total detectable anions) followed by the second abundant  $\text{SO}_4^{2-}$  with 35.9% anionic contribution, and the  $\text{Cl}^-$  and  $\text{F}^-$  accounted for 14.6% and 2.4% of the total anions (Fig. 3a). These results are different from most previous studies that  $\text{SO}_4^{2-}$  predominate the rainwater anions (Keresztesi

et al., 2019). It reflects the achievement of atmospheric  $\text{SO}_2$  emission reduction/control, and also the relative emission intensity of nitrogen oxide and sulfur oxide pollutants, which can be supported by the increasing ratios of atmospheric  $\text{NO}_2$  and  $\text{SO}_2$  concentrations (Fig. 2c) (Sun et al., 2021). In contrast,  $\text{NH}_4^+$  was the most abundant cation and  $\text{Ca}^{2+}$  was the following one, contributed 68.6% and 14.6% of the total cations, respectively, while the percentage of  $\text{Mg}^{2+}$  (8.9%),  $\text{Na}^+$  (5.9%), and  $\text{K}^+$  (2.0%) were limited (Fig. 3b). Overall, these four ions ( $\text{NO}_3^-$ ,  $\text{SO}_4^{2-}$ ,  $\text{NH}_4^+$ , and  $\text{Ca}^{2+}$ ) accounted for more than 80% of the total ions. From the perspective of historical variations (Fig. 3c), the proportion of acid ion  $\text{SO}_4^{2-}$  showed a significant decreasing trend, while that of  $\text{NO}_3^-$  fluctuated in a wide range which presented the highest percentage of  $\text{NO}_3^-$  in 2021 extreme rainfall period. The proportion of alkaline ion  $\text{NH}_4^+$  reflected an increasing trend from 1995 to 2021 with the highest percentage of 68.6% in study period, and  $\text{Ca}^{2+}$  proportion fluctuated among these years. It is noteworthy that the proportions of rainwater  $\text{K}^+$  and  $\text{Na}^+$  were relatively higher, indicating the important potential contribution of biomass combustion on rainwater chemicals (Xu et al., 2020).

##### 3.1.2. Daily variations

On the daily scale, the rainwater pH varied slightly during study period, while the EC variations were significantly and the high EC values were often accompanied with low rainfall amount (Fig. 4a). As shown in Fig. 4b and c, the highest total cation (1565  $\mu\text{eq L}^{-1}$ ) and anion (782.8  $\mu\text{eq L}^{-1}$ ) concentration was observed on 26 July with the lowest precipitation amount (0.7 mm). The rainwater ion concentration was generally higher on the first day of each rainfall event (>2d event) and tend to decrease on the following days, such as 11 July, 17 July, and 26 July (Fig. 4b and c). The daily rainwater ion concentrations were not significantly related to the concentrations of atmospheric pollutants ( $\text{SO}_2$ ,  $\text{NO}_2$ ,  $\text{PM}_{2.5}$ , and  $\text{PM}_{10}$ ). However, the atmospheric  $\text{PM}_{2.5}$  and  $\text{PM}_{10}$  concentrations presented similar variations (Fig. 4b). In contrast, the daily variation of  $\text{NO}_2$  was more obvious than that of  $\text{SO}_2$  (Fig. 4c), indicating the differences of various potential emission sources contribution of these two pollutants on daily scale (Zeng et al., 2020b).

##### 3.1.3. Rainfall scouring processes

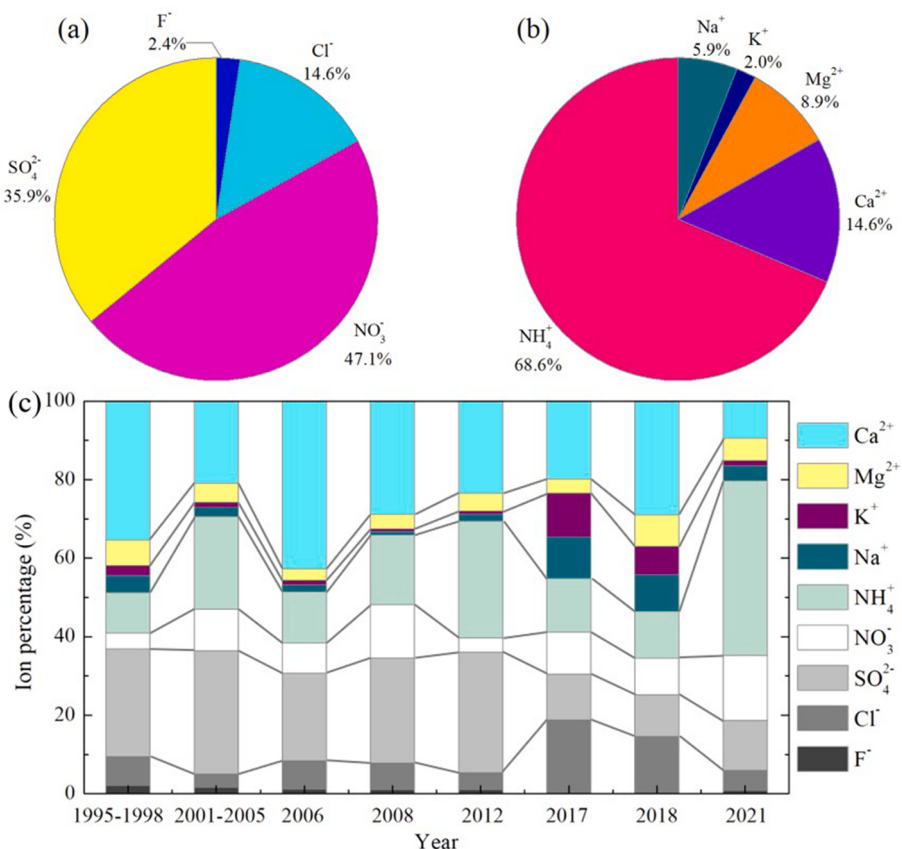
The rain-scorer effect is one of the most important pathways of atmospheric pollutants remove. The daily precipitation amount and major ion concentrations ( $\text{NO}_3^-$ ,  $\text{SO}_4^{2-}$ ,  $\text{NH}_4^+$ ,  $\text{Ca}^{2+}$ , and  $\text{Mg}^{2+}$ ) of rainwater were analyzed via fitting to clarify the scouring processes (Fig. 5). The clear negative logarithmic relationships were found between these ions concentrations and daily precipitation amount. That is, the rainwater  $\text{NO}_3^-$ ,  $\text{SO}_4^{2-}$ ,  $\text{NH}_4^+$ ,  $\text{Ca}^{2+}$ , and  $\text{Mg}^{2+}$  concentrations were higher when rainfall amount is smaller, whereas lower if rainfall amount is large. These findings reflected that the atmospheric acidic/alkaline matters were well removed by rainwater scouring, for example, gaseous  $\text{SO}_x$  and  $\text{NO}_x$ , nitrate aerosol, aerosol/gaseous ammonia, and  $\text{Ca}/\text{Mg}$ -bearing particulate, which were in agreement with the commonly results in

Table 1

Overview of EC, pH, and ionic concentrations of rainwater in Beijing during the 2021 extreme rainfall period and the reported data from 1995 to 2018.

Year	Parameters	EC	pH	$\text{F}^-$	$\text{Cl}^-$	$\text{SO}_4^{2-}$	$\text{NO}_3^-$	$\text{NH}_4^+$	$\text{Na}^+$	$\text{K}^+$	$\text{Mg}^{2+}$	$\text{Ca}^{2+}$
2021 This work	VWM	47	6.9	3.6	22.1	54.5	71.5	191.8	16.6	5.6	24.8	40.7
	Min	15	6.5	1.0	13.9	19.2	18.1	35.1	0.0	0.0	10.4	6.4
	Max	157	7.5	11.5	251.5	203.1	317.9	476.6	238.1	92.3	122.7	737.5
	Mean	60	7.0	4.1	35.9	67.4	103.8	221.1	25.6	11.1	32.3	92.9
	Median	59	7.0	2.8	19.8	56.0	80.5	253.1	13.7	7.1	24.8	41.8
1995–1998	VWM	–	6.9	26.9	97.2	359.0	54.5	135.0	57.2	33.3	86.0	464.0
2001–2005	VWM	–	6.0	15.4	34.9	314.0	106.0	236.0	22.5	13.8	48.4	209.0
2006	VWM	77	5.1	15.7	104.0	315.8	109.0	185.6	25.0	17.7	40.4	607.2
2008	VWM	73	5.3	10.5	67.8	270.0	139.0	179.0	8.5	6.7	38.5	291.0
2012	VWM	82	4.9	12.0	50.9	357.0	42.6	346.0	21.5	9.2	53.3	273.0
2017	VWM	49	6.7	–	123.4	77.2	70.2	89.9	69.2	74.0	23.7	130.3
2018	VWM	38	6.8	–	76.8	55.4	49.1	62.7	49.3	38.0	42.3	152.4

Note: The unit of EC is  $\mu\text{S cm}^{-1}$ , the unit of each ion is  $\mu\text{eq L}^{-1}$ . Data are from: 1995–1998 (Feng et al., 2001), 2001–2005 (Yang et al., 2012), 2006 (Xu and Han, 2009), 2008 (Xu et al., 2012), 2012 (Xu et al., 2015), 2017 and 2018 (Xu et al., 2020).



**Fig. 3.** The Rainwater ion composition percentages in Beijing during the extreme rainfall period: (a) anion percentages; (b) cation percentages; and (c) historical change of ion composition percentages. The references in 1995–2018 are same to Table 1.

previous publications (Szép et al., 2018). In washing process, the atmospheric matters are strongly and effectively washed down during the early rain-stage, resulting in high ion contents in rainwater with the lower rainfall amount, that is, below-cloud processes. However, as the continuous progress of rainfall event, the rainwater ion concentrations decreased and eventually stabilized at a low concentration level due to lack of continuous supplements of atmospheric substance (Ge et al., 2021). This could also explain the observed higher ion concentration on the first day of a sustained rainfall event in Fig. 4. It should be noted that the ion concentrations of  $\text{NO}_3^-$ ,  $\text{SO}_4^{2-}$ ,  $\text{NH}_4^+$ ,  $\text{Ca}^{2+}$ , and  $\text{Mg}^{2+}$  altered in a stable range after the daily precipitation amount reached  $\sim 15$  mm (Fig. 5, dark box), that is, the atmospheric matters were almost completely washed down under this rainfall condition ( $> 15$  mm). In this case, the ionic concentrations of rainwater and the cloud water/droplet are similar, revealing the in-cloud process (Rao et al., 2017). Moreover, the significant increase of rainwater  $\text{NH}_4^+$  concentration observed in the 45 mm rainfall amount, can be interpreted by the irregular nonagricultural emissions (e.g., vehicle emissions) of  $\text{NH}_3$  in urban region (Gu et al., 2022), which will be further discussed in the source identification. In addition, the dilution effect is negligible when precipitation amount exceed 15 mm, while the long-distance transportation of air pollutants can also be a significant potential contributor of rainwater ion compositions via in-cloud process. In contrast, the rainwater ion concentrations varied significantly when the precipitation amount is  $< 15$  mm (Fig. 5), implying the intense below-cloud rainfall scavenging.

### 3.2. Rainwater neutralizing capacity during extreme rainfall period

As mentioned above, all rainwater samples have the pH value exceed 6.5 during the extreme rainfall period. Obviously, all pH values were greater than the “natural rainwater acidity” (the dissolved natural  $\text{NO}_x$ ,

$\text{SO}_x$ , and  $\text{CO}_2$  in rain droplets gives rainwater a pH around 5.0–5.6 in natural atmosphere). Generally, the rainwater acidity is controlled primarily by the inputs of acidic ions ( $\text{SO}_4^{2-}$  and  $\text{NO}_3^-$ ) (Zhou et al., 2019). Therefore, there are two main reasons for the high pH of rainwater (low acidity): (1) lack of acidic ions input; and (2) alkaline substances input and neutralized acidic materials. However, the rainwater  $\text{SO}_4^{2-}$  and  $\text{NO}_3^-$  concentrations were not very low (Table 1), suggesting that the lack of acidic ions is not responsible for the high pH values of rainwater during extreme rainfall period in Beijing, while the neutralizing process is. Previous studies have confirmed that the basic ions were the most important contributors of rainwater neutralizing capacity (Wu et al., 2016). The fractional acidity (FA) is calculated to examine the overall neutralizing status as equation (2) (Wu et al., 2012). Based on the VWM concentrations of rainwater ions, the FA is calculated to be 0.0011 in the study period, indicating that 99.89% of the  $\text{NO}_3^-$  and  $\text{SO}_4^{2-}$  derived rainwater acidity was neutralized by alkaline components. The neutralizing capacity observed in Beijing extreme rainfall period is much stronger than the mean level in Europe, where alkaline ion neutralized 70% of rainwater acidity with the FA value of 0.3 (Keresztesi et al., 2019).

In order to assess the neutralizing capacity of each alkaline ion in rainwater, the neutralization factor (NF) was examined as equation (3). As shown in Fig. 6a, the NF values of rainwater  $\text{NH}_4^+$ ,  $\text{Na}^+$ ,  $\text{K}^+$ ,  $\text{Mg}^{2+}$ , and  $\text{Ca}^{2+}$  during 2021 extreme rainfall period in Beijing were 1.52, 0.13, 0.04, 0.20, and 0.32, respectively. These results reflected that  $\text{NH}_4^+$  was the primary neutralizing alkaline ion, and  $\text{Ca}^{2+}$  was the secondary contributor to rainwater neutralizing process, while the neutralization contribution of the rest alkaline ions were very limited. There are some differences from previous studies in Beijing during 1995–2018 (Fig. 6a), where the neutralizing capacity of  $\text{Ca}^{2+}$  was usually dominant in rainwater neutralizing process. Moreover, the overall contribution of

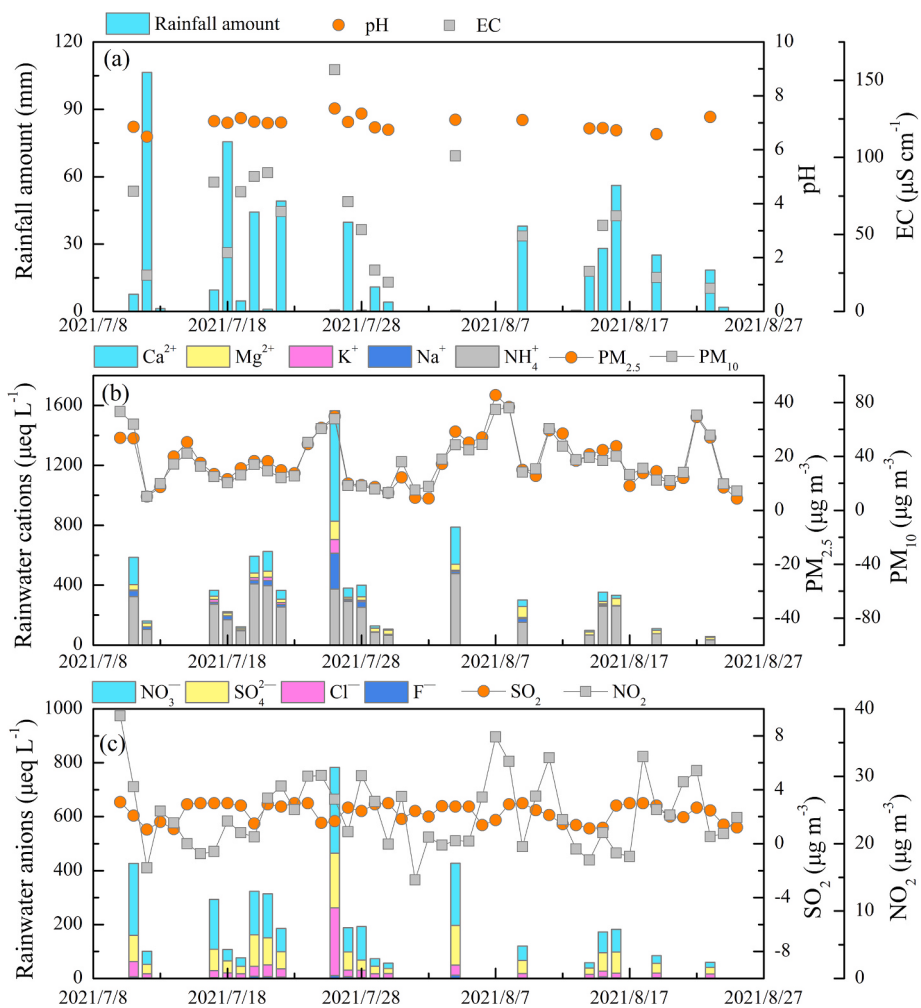


**Fig. 4.** The daily variations of: (a) rainwater pH and EC, rainfall amount; (b) rainwater cations concentrations, atmospheric PM<sub>2.5</sub> and PM<sub>10</sub> concentrations; (c) rainwater anions concentrations, atmospheric SO<sub>2</sub> and NO<sub>2</sub> concentrations in Beijing during the extreme rainfall period. The data of atmospheric pollutants concentrations are from Haidian Wanliu monitoring station reported by Beijing Municipal Ecological Environmental Monitoring Center.

NF-NH<sub>4</sub><sup>+</sup> to the total NFs increased gradually from 1995 to 2021 (Fig. 6a). Compared to the developed countries with the highest NF value of Na<sup>+</sup> (average NF = 0.54) and the secondary NF value of NH<sub>4</sub><sup>+</sup> (average NF = 0.46) (Keresztesi et al., 2019), the findings in Beijing implying the widespread inputs of possible ammonia sources to rainwater during the extreme rainfall period. To evaluate and compare the major neutralization capacity of alkaline constituents, the neutralizing and acidifying potential ratios (NP/AP) were calculated and presented in Fig. 6b, the NP/AP ratios of other Chinese cities were also plotted. The NP/AP ratios and pH values in Beijing (1995–2021) were basically remained at the medium level. The rainwater NP/AP ratios of Beijing rainwater were significantly lower than that of Qinghai (3.91) (Zhang et al., 2003) and Lanzhou (3.63) (Xu et al., 2009) in Northwest China, indicating the important contributions of Ca-bearing alkaline constituents originated from atmospheric dusts in northwest China on the intense neutralizing capacity. However, the major neutralization capacity of rainwater in Beijing was relatively higher than that in South China cities with high acid rain frequency, such as Guangzhou (Cao et al., 2009), Shanghai (Huang et al., 2008), Guiyang (Han et al., 2011), Chengdu (Wang and Han, 2011), Jinhua (Zhang et al., 2007), and Shenzhen (Zhou et al., 2019) where the rainwater SO<sub>4</sub><sup>2-</sup> concentrations exhibited high level (95–238 µeq L<sup>-1</sup>). In combined with the assessed results of the FA, NF, and NP/AP of rainwater and the invariably high concentration level of rainwater NH<sub>4</sub><sup>+</sup> in Beijing (Table 1), here we attributed the high pH of rainwater (relative strong neutralizing

capacity) mainly to the contribution of ammonia-containing substances.

### 3.3. Source of rainwater components

#### 3.3.1. Source identification

The correlation analysis presented significantly positive correlation ( $p < 0.05$ ) among almost all rainwater ions, such as SO<sub>4</sub><sup>2-</sup> and NO<sub>3</sub><sup>-</sup> ( $R = 0.91, p < 0.01$ ), NH<sub>4</sub><sup>+</sup> and NO<sub>3</sub><sup>-</sup> ( $R = 0.84, p < 0.01$ ) (Fig. S2). Therefore, although the correlation analysis can reflect the potential co-sources and similar chemical processes of rainwater ions (Naimabadi et al., 2018), it is quite hard to clarify the sources information of rainwater components in Beijing by correlation analysis. For this, the ternary diagrams of rainwater components were applied to present the relative variations and qualitative sources analysis of rainwater ions. In the anionic ternary diagram (Fig. 7a), the sea salt-controlled rainwater was generally plotted on the end of [Cl<sup>-</sup>], such as the observed marine island rainwater in Yongxing Island (South China Sea) (Xiao et al., 2016), while the human activities-influenced rainwater was usually distributed on the line between [NO<sub>3</sub><sup>-</sup>] and [SO<sub>4</sub><sup>2-</sup>] due to regional emissions and/or long-distance transportation of NO<sub>x</sub> and SO<sub>x</sub> (Zeng et al., 2019). During the study period, rainwater samples were scattered near the [NO<sub>3</sub><sup>-</sup>] and [SO<sub>4</sub><sup>2-</sup>] line with a slightly trend to the end of [Cl<sup>-</sup>], and all samples were relatively closer to the end of [NO<sub>3</sub><sup>-</sup>] (Fig. 7a), indicating that the rainwater anions were controlled by human inputs, in particular the mobile source emissions (mainly motor emissions), while the influence of sea

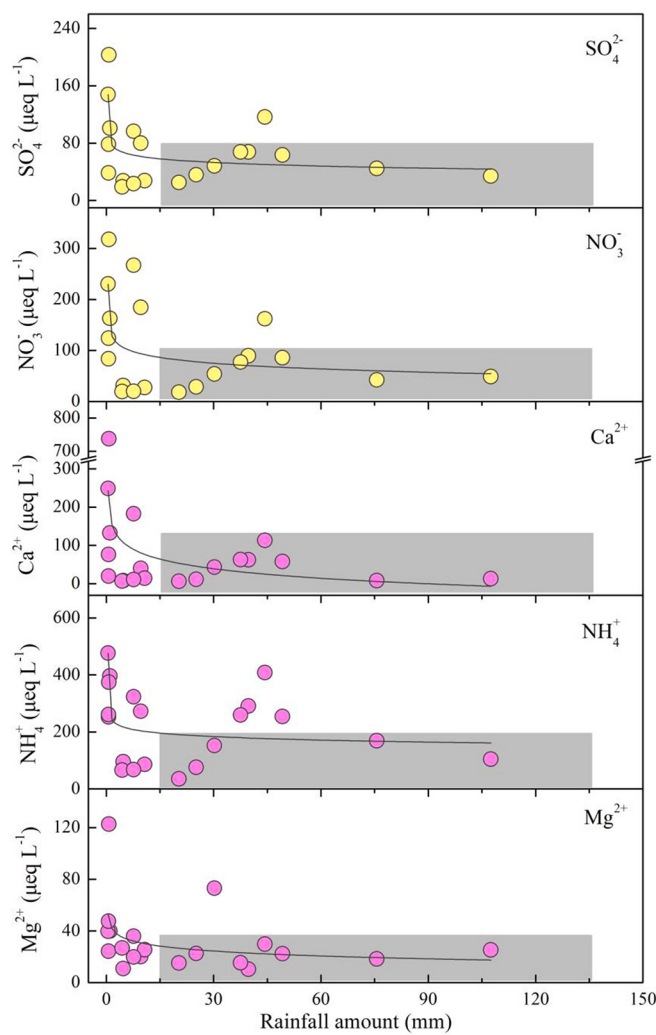


**Fig. 5.** The relationship between rainfall amount and ion concentrations reveals the rainfall-scour effect of atmospheric matters. The rainfall amount data are from the Weather China (<http://www.weather.com.cn/>).

salt input on rainwater anions were very limited. This phenomenon is quite different from the rainwater observed results from Chinese desert (Rao et al., 2017), forest (Han et al., 2010), agricultural area (Zeng et al., 2020c), and previous Beijing (2012) (Xu et al., 2015), where the fixed emission sources dominated the rainwater anions. This reflected the

achievement of atmospheric  $\text{SO}_2$  emission reduction/control and the high intensity of transportation pollution (supported by the high motor vehicles number) in such a megacity. That is, the transportation-emitted  $\text{NO}_x$  is the leading role of human emissions, whereas the industrial activities that discharge  $\text{SO}_2$  in urban Beijing are relatively weak. Thus, the regional transportation emissions controlled the rainwater anionic compositions. Furthermore, in cationic ternary diagram (Fig. 7b), the rainwater samples controlled by crust input, dominated by sea salt input, and influenced by human activities were plotted on the end of  $[\text{Ca}^{2+} + \text{Mg}^{2+}]$ ,  $[\text{Na}^+ + \text{K}^+]$ , and  $[\text{NH}_4^+]$  (Zeng et al., 2020c), respectively. The observed rainwater cations during 2021 extreme rainfall period in Beijing mainly presented the co-contributions of anthropogenic emissions (e.g., municipal wastes/feces emission) and the crustal materials input (Keresztesi et al., 2020), while the sea salt contribution was negligible (Fig. 7b).

As shown in Fig. 8, the relationships of typical ion equivalent ratios ( $\text{SO}_4^{2-}/\text{Na}^+$ ,  $\text{NO}_3^-/\text{Na}^+$ ,  $\text{NH}_4^+/\text{Na}^+$  and  $\text{Cl}^-/\text{Na}^+$ ;  $\text{Mg}^{2+}/\text{Ca}^{2+}$  and  $\text{SO}_4^{2-}/\text{Ca}^{2+}$ ) of rainwater during study period in Beijing were used to determine the possible sources of rainwater ions. Different from the rainwater in carbonate rock area (Zeng et al., 2020c), only few rainwater samples (Beijing, 2021) presented low  $\text{Cl}^-/\text{Na}^+$  ratio (<1), while  $\text{Cl}^-/\text{Na}^+$  ratios of most samples were higher than that of seawater (Berner and Berner, 1987) (Fig. 8a). In combined with the low concentrations of rainwater  $\text{Cl}^-$  and  $\text{Na}^+$ , it can be considered that the sea salt input materials has been partly depleted during the atmospheric cloud transported processes. The  $\text{SO}_4^{2-}/\text{Na}^+$  ratios of half of the rainwater samples and the  $\text{NO}_3^-/\text{Na}^+$  ratios of most rainwater samples were higher (Fig. 8a and b), indicating the significant influence of anthropogenic inputs on rainwater components. That is, these anions ( $\text{SO}_4^{2-}$  and  $\text{NO}_3^-$ ) primarily originated from human emissions (Naimabadi et al., 2018), which further support the above discussion of anionic ternary diagram. Moreover, almost all rainwater samples presented a  $\text{NO}_3^-/\text{SO}_4^{2-}$  ratio exceed 1, suggesting the relatively low contribution of fixed emission sources (e.g., regional coal combustion) during the study period (Li et al., 2020). It can also be supported by the historical comparison with previous Beijing rainwater with high  $\text{SO}_4^{2-}/\text{Na}^+$  ratios during 2006–2012 (Fig. 8a), and by the trend of  $\text{NO}_2$  and  $\text{SO}_2$  discharge ratios (Fig. 2c). In addition, we also observed high  $\text{NH}_4^+/\text{Na}^+$  ratios (~10, even up to 106) relative to the  $\text{Cl}^-/\text{Na}^+$  ratio (Fig. 8c) and high  $\text{NH}_4^+/\text{NO}_3^-$  ratios (~2.1, up to 4.0), indicating plentiful anthropogenic ammonia inputs. As a possible interpretation, previous studies confirmed that municipal wastes/feces could produce the gaseous  $\text{NH}_3$  (Sun et al., 2021) and the nonagricultural emissions (mainly vehicle emissions) dominated the  $\text{NH}_3$  sources in urban atmosphere of Beijing (Gu et al., 2022), which could be the significant sources of rainwater  $\text{NH}_4^+$ . Moreover, a long-term observation in North China also showed a higher contribution rate of fossil fuel burning to atmospheric ammonia in urban

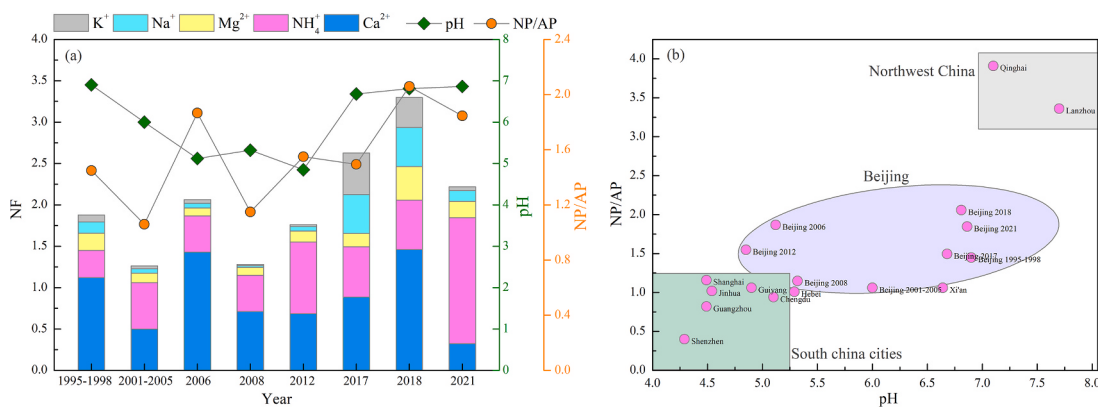


**Fig. 6.** (a) The historical change of neutralization factors (NFs), pH, and (b) the ratio of neutralizing potential to acidifying potential (NP/AP). The references of Beijing in 1995–2018 are same to Table 1; The data of other areas are from: Qinghai (Zhang et al., 2003), Lanzhou (Xu et al., 2009), Guangzhou (Cao et al., 2009), Shanghai (Huang et al., 2008), Guiyang (Han et al., 2011), Chengdu (Wang and Han, 2011), Jinhua (Zhang et al., 2007), and Shenzhen (Zhou et al., 2019).

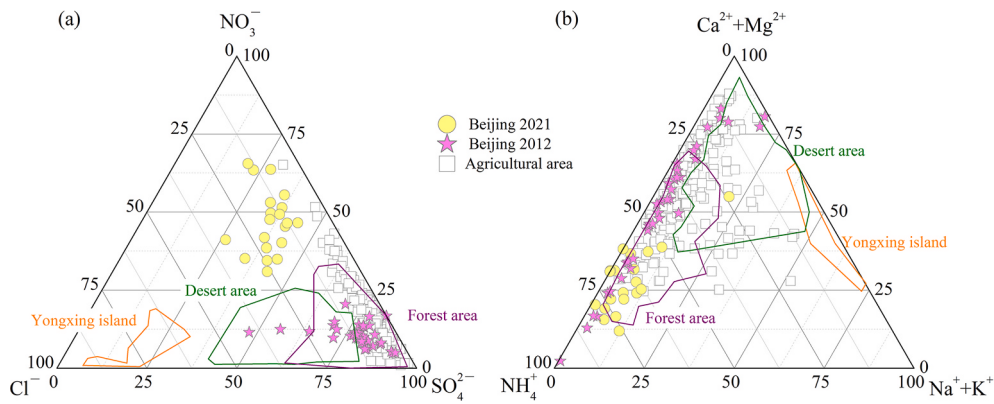


**Fig. 7.** Ternary diagrams of major ions of rainwater in Beijing: (a) anions, (b) cations. The rainwater ion compositions of other regions in China are also presented (Han et al., 2010; Xu et al., 2015; Xiao et al., 2016; Rao et al., 2017; Zeng et al., 2020c).

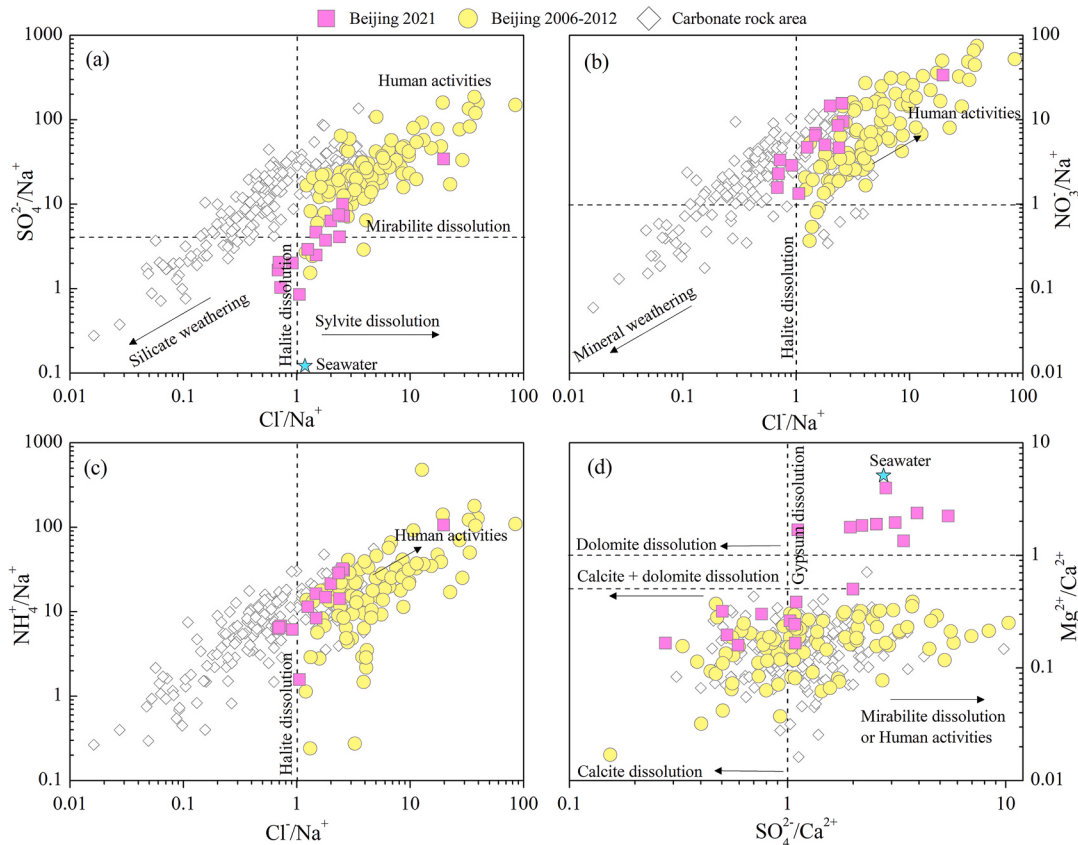


**Fig. 8.** The characteristic ion equivalent ratios of Beijing rainwater during the rainy season in 2021 and 2006–2012.

region than in rural area due to dense population and traffic flow (Feng et al., 2022), which also accounts for rainwater  $\text{NH}_4^+$  source to a certain extent. In Fig. 8d, the  $\text{Mg}^{2+}/\text{Ca}^{2+}$  ratios of rainwater ranged between 0.2–4.0 (higher than the  $\text{Mg}^{2+}/\text{Ca}^{2+}$  ratios of previous rainwater in Beijing), reflecting the influence of atmospheric dust on rainwater  $\text{Ca}^{2+}$  and  $\text{Mg}^{2+}$  during the crust input processes with differential weathering of calcite and dolomite. Although the concentrations of  $\text{F}^-$  and  $\text{K}^+$  are very low in rainwater samples (Table 1), the crust input (e.g., sylvite and silicate weathering) and fluoride-related industry (Zeng and Han, 2021) can also be the potential human sources of rainwater  $\text{K}^+$  and  $\text{F}^-$  (Khare et al., 2004).

### 3.3.2. Source contribution

According to the above discussion, here we defined three major

contributed sources of rainwater components, including sea salt input (SSI), crust dust input (CDI), and human input (HI). The relative contribution of each sources are calculated based on reasonable assumptions (that is, all  $\text{Na}^+$  is only from sea salt,  $\text{NH}_4^+$  and  $\text{F}^-$  are only contributed by human source,  $\text{Cl}^-$  has no crust contribution, and human input  $\text{K}^+$ ,  $\text{Mg}^{2+}$ ,  $\text{Ca}^{2+}$  are negligible (Rao et al., 2017)) as follows:

$$\text{SSI (\%)} = [100 \times \text{Na}^+_{\text{rainwater}} \times (\text{X}/\text{Na}^+)_{\text{seawater}}]/X_{\text{rainwater}} \quad (5)$$

$$\text{CDI (\%)} = [100 \times \text{Ca}^{2+}_{\text{rainwater}} \times (\text{X}/\text{Ca}^{2+})_{\text{crust}}]/X_{\text{rainwater}} \quad (6)$$

$$\text{HI (\%)} = 100 - \text{SSI} - \text{CDI} \quad (7)$$

where the  $\text{Na}^+_{\text{rainwater}}$  and  $\text{Ca}^{2+}_{\text{rainwater}}$  are the concentrations of rainwater  $\text{Na}^+$  and  $\text{Ca}^{2+}$ ,  $(\text{X}/\text{Na}^+)_{\text{seawater}}$  and  $(\text{X}/\text{Ca}^{2+})_{\text{crust}}$  are the ratio of X

to  $\text{Na}^+$  in seawater (Berner and Berner, 1987) and the ratio of X to  $\text{Ca}^{2+}$  in crust (Wang and Han, 2011), and  $X_{\text{rainwater}}$  is the concentrations of X in rainwater.

As shown in Fig. 9 and Table S1, the vast majorities of rainwater  $\text{SO}_4^{2-}$  and  $\text{NO}_3^-$  were derived from human input with the contribution of 94.9% and 99.9%, while the sea salt and crust dust contributed 3.7% and 1.4% of  $\text{SO}_4^{2-}$ . 86.9% of rainwater  $\text{Cl}^-$  originated from sea salt input and 13.1% of rainwater  $\text{Cl}^-$  was from human input. The rainwater  $\text{K}^+$ ,  $\text{Mg}^{2+}$ ,  $\text{Ca}^{2+}$  were primarily from crust dust input with the contribution of 94.0%, 92.3%, and 98.2%, while the sea salt provided 6.0% of  $\text{K}^+$ , 7.7% of  $\text{Mg}^{2+}$  and 1.8% of  $\text{Ca}^{2+}$ , respectively.

### 3.4. Environmental implication

As comparison with other cities over China, although the Beijing rainwater was relatively well neutralized, the rainfall deposited nitrate/sulfate incorporated with the  $\text{H}^+$  in the surface water systems can drive the acidification of surface water, which has been the significant focus of environmental studies (Chen et al., 2019). Therefore, the concentration levels of sulfate and nitrate in rainwater are the important reflection of the potential impacts of rainfall processes on surface water environment to a certain extent, such as the influence on weathering process of earth-surface and the further impact on global climate change. Moreover, the dominated type of rainwater acidification in most areas of northern China has steadily changed from sulfuric acid to the mixed type controlled by nitrate and sulfate ( $S/N = 0.5\text{--}1.5$ ) since 2015 (Liu et al., 2020), thus the observed higher nitrate deposition (with increased potential impact relative to sulfuric ion) in Beijing during the extreme rainfall period needs more attention. In addition, given that the urban river channels in Tongzhou District (Beijing) are the main rivers (~90%) that receiving urban flood during the extreme rainfall period (Liu et al., 2021), further spatial-temporal observation of rainwater chemistry together with the river water chemistry in these urban river channels are of great significance for better understanding of the environmental implications of extreme rainfall processes on earth-surface.

## 4. Conclusions

In brief, daily-scale rainwater samples across the whole 2021 extreme rainfall period in megacity Beijing were collected to clarify the rainwater chemical evolution, sources and potential environmental effects. The stoichiometry-based and historical comparison of rainwater chemical components effectively reflected the atmospheric substance scouring process, neutralizing process, and the origins of rainwater ions. The primary rainwater ions were  $\text{NH}_4^+$ ,  $\text{NO}_3^-$ ,  $\text{SO}_4^{2-}$ , and  $\text{Ca}^{2+}$  with distinctly daily variations, which can be well removed by rain-scour process. The overall rainwater neutralization level is relatively high, presented the high value of neutralization factor (NF, with largest contribution of  $\text{NH}_4^+$ ) and ratio of neutralizing and acidifying potential (NP/AP). Source identification revealed that human input contributed majorities of rainwater  $\text{SO}_4^{2-}$  (94.9%) and  $\text{NO}_3^-$  (99.9%), sea salt input was the major source of  $\text{Cl}^-$  (86.9%) and all  $\text{Na}^+$ , while the rainwater  $\text{K}^+$ ,  $\text{Mg}^{2+}$ ,  $\text{Ca}^{2+}$  were mainly derived from crust dust input with the contribution of 94.0%, 92.3%, and 98.2%. Rainwater  $\text{NH}_4^+$  was considered only to be originated from anthropogenic sources, such as municipal wastes/feces, vehicle emission and fossil fuel burning. Our research emphasizes the influence of extreme rainfall on urban environment from the perspective of rainwater chemical evolution, which would be beneficial for better urban environmental protection, particularly the air environment under the background of climate change in megacity. Moreover, given that only the daily-scale rainwater samples were studied in this work, the influence of rainfall intensity was not taken into account, however, the significant differences in rainfall intensity on the hourly scale were generally observed in individual extreme rainfall event. Therefore, the higher frequency/time-resolution sampling (e.g., sequential sampling technique) of rainwater in representative extreme

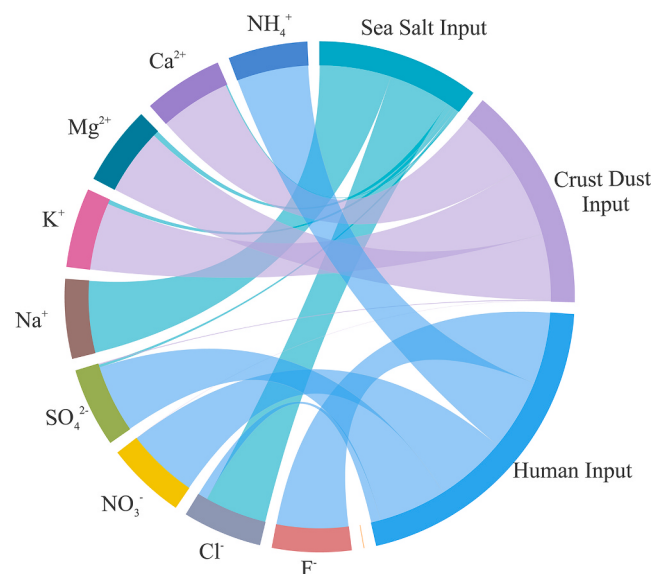


Fig. 9. The relative contributions of sea salt input, crust dust input, and human input to rainwater ions in Beijing during the extreme rainfall period.

rainfall event is needed in the further study to catch the rainwater chemical evolution during each event.

## CRediT authorship contribution statement

**Jie Zeng:** Conceptualization, Investigation, Data curation, Methodology, Writing – original draft, Writing – review & editing, All authors read and approved the final manuscript. **Guilin Han:** Conceptualization, Investigation, Data curation, Methodology, Resources, Writing – original draft, Writing – review & editing, Funding acquisition, All authors read and approved the final manuscript. **Shitong Zhang:** Investigation, Writing – original draft, All authors read and approved the final manuscript. **Xuhuan Xiao:** Investigation, Methodology, All authors read and approved the final manuscript. **Yikai Li:** Investigation, Methodology, All authors read and approved the final manuscript. **Xi Gao:** Investigation, Methodology, All authors read and approved the final manuscript. **Di Wang:** Investigation, Methodology, All authors read and approved the final manuscript. **Rui Qu:** Data curation, Investigation, All authors read and approved the final manuscript.

## Declaration of competing interest

The authors declare that they have no known competing financial interests or personal relationships that could have appeared to influence the work reported in this paper.

## Data availability

Data will be made available on request.

## Acknowledgments

This work was supported by the National Natural Science Foundation of China (No.41661144029 and No.41325010), and also supported by the "Double Hundred Action Plan" College Students Social Practice Project (Jie Zeng) organized by the Beijing Municipal Education Commission.

## Appendix A. Supplementary data

Supplementary data to this article can be found online at <https://doi.org/10.1016/j.jclepro.2022.133732>.

[org/10.1016/j.jclepro.2022.133732](https://doi.org/10.1016/j.jclepro.2022.133732).

## References

- Arnbjerg-Nielsen, K., Willems, P., Olsson, J., Beecham, S., Pathirana, A., Bülow Gregersen, I., Madsen, H., Nguyen, V.-T.-V., 2013. Impacts of climate change on rainfall extremes and urban drainage systems: a review. *Water Sci. Technol.* 68, 16–28.
- Berner, E.K., Berner, R.A., 1987. Global Water Cycle: Geochemistry and Environment. Prentice-Hall, New York.
- Cao, Y.-Z., Wang, S., Zhang, G., Luo, J., Lu, S., 2009. Chemical characteristics of wet precipitation at an urban site of Guangzhou, South China. *Atmos. Res.* 94, 462–469.
- Chen, Z., Huang, T., Huang, X., Han, X., Yang, H., Cai, Z., Yao, L., Han, X., Zhang, M., Huang, C., 2019. Characteristics, sources and environmental implications of atmospheric wet nitrogen and sulfur deposition in Yangtze River Delta. *Atmos. Environ.* 219, 116904.
- Feng, S., Xu, W., Cheng, M., Ma, Y., Wu, L., Kang, J., Wang, K., Tang, A., Collett, J.L., Fang, Y., Goulding, K., Liu, X., Zhang, F., 2022. Overlooked nonagricultural and wintertime agricultural NH<sub>3</sub> emissions in quzhou county, north China plain: evidence from 15N-stable isotopes. *Environ. Sci. Technol. Lett.* 9, 127–133.
- Feng, Z., Huang, Y., Feng, Y., Ogura, N., Zhang, F., 2001. Chemical composition of precipitation in beijing area, northern China. *Water Air Soil Pollut.* 125, 345–356.
- Ge, B., Xu, D., Wild, O., Yao, X., Wang, J., Chen, X., Tan, Q., Pan, X., Wang, Z., 2021. Inter-annual variations of wet deposition in Beijing from 2014–2017: implications of below-cloud scavenging of inorganic aerosols. *Atmos. Chem. Phys.* 21, 9441–9454.
- Gu, M., Pan, Y., Sun, Q., Walters, W.W., Song, L., Fang, Y., 2022. Is fertilization the dominant source of ammonia in the urban atmosphere? *Sci. Total Environ.* 838 (1), 155890.
- Han, G., Song, Z., Tang, Y., Wu, Q., Wang, Z., 2019. Ca and Sr isotope compositions of rainwater from Guiyang city, Southwest China: implication for the sources of atmospheric aerosols and their seasonal variations. *Atmos. Environ.* 214, 116854.
- Han, G., Tang, Y., Wu, Q., Tan, Q., 2010. Chemical and strontium isotope characterization of rainwater in karst virgin forest, Southwest China. *Atmos. Environ.* 44, 174–181.
- Han, G., Wu, Q., Tang, Y., 2011. Acid rain and alkalization in southwestern China: chemical and strontium isotope evidence in rainwater from Guiyang. *J. Atmos. Chem.* 68, 139–155.
- Huang, K., Zhuang, G., Xu, C., Wang, Y., Tang, A., 2008. The chemistry of the severe acidic precipitation in Shanghai, China. *Atmos. Res.* 89, 149–160.
- Jaspriet, K., Charu, J., 2021. Urban air pollution and human health: a review. *Curr. World Environ.* 16, 362–377.
- Keresztesi, Á., Birsan, M.-V., Nita, I.-A., Bodor, Z., Szép, R., 2019. Assessing the neutralisation, wet deposition and source contributions of the precipitation chemistry over Europe during 2000–2017. *Environ. Sci. Eur.* 31, 50.
- Keresztesi, Á., Nita, I.-A., Birsan, M.-V., Bodor, Z., Pernyeszi, T., Micheu, M.M., Szép, R., 2020. Assessing the variations in the chemical composition of rainwater and air masses using the zonal and meridional index. *Atmos. Res.* 237, 104846.
- Khare, Puja, Goel, Ankur, Patel, Devendra, Behari, Jairaj, 2004. Chemical characterization of rainwater at a developing urban habitat of Northern India. *Atmos. Res.* 69, 135–145.
- Li, C., Li, S.-L., Yue, F.-J., He, S.-N., Shi, Z.-B., Di, C.-L., Liu, C.-Q., 2020. Nitrate sources and formation of rainwater constrained by nitrate isotopes in Southeast Asia: example from Singapore. *Chemosphere* 241, 125024.
- Li, J., Xu, X.-d., Li, Y.-q., Zhao, T.-l., Wu, C., 2021. The key supply source of long-distance moisture transport for the extreme rainfall event on july 21, 2012 in beijing. *J. Trop. Meteorol.* 27, 34.
- Li, Y., Ma, C., Wang, Y., 2019. Landslides and debris flows caused by an extreme rainfall storm on 21 July 2012 in mountains near Beijing, China. *Bull. Eng. Geol. Environ.* 78, 1265–1280.
- Liu, M., Song, Y., Xu, T., Xu, Z., Wang, T., Yin, L., Jia, X., Tang, J., 2020. Trends of precipitation acidification and determining factors in China during 2006–2015. *J. Geophys. Res. Atmos.* 125, e2019JD031301.
- Liu, Y.-M., Yang, S.-N., Wang, Y.-T., Liu, X.-Y., Zhang, X.-W., Zhu, Y.-Y., 2021. Flood simulation and verification in Beijing urbanarea based on CADDIES-2D model. *Water Resour. Power* 39, 107–110 (in Chinese).
- Naimabadi, A., Shirmardi, M., Maleki, H., Teymouri, P., Goudarzi, G., Shahsavani, A., Sorooshian, A., Babaei, A.A., Mehrabi, N., Baneshi, M.M., Zarei, M.R., Lababpour, A., Ghozikali, M.G., 2018. On the chemical nature of precipitation in a populated Middle Eastern Region (Ahvaz, Iran) with diverse sources. *Ecotoxicol. Environ. Saf.* 163, 558–566.
- Qin, C., Li, S.-L., Waldron, S., Yue, F.-J., Wang, Z.-J., Zhong, J., Ding, H., Liu, C.-Q., 2020. High-frequency monitoring reveals how hydrochemistry and dissolved carbon respond to rainstorms at a karstic critical zone, Southwestern China. *Sci. Total Environ.* 136833.
- Rao, W., Han, G., Tan, H., Jin, K., Wang, S., Chen, T., 2017. Chemical and Sr isotopic characteristics of rainwater on the Alxa Desert Plateau, North China: implication for air quality and ion sources. *Atmos. Res.* 193, 163–172.
- Sun, S., Liu, S., Li, L., Zhao, W., 2021. Components, acidification characteristics, and sources of atmospheric precipitation in Beijing from 1997 to 2020. *Atmos. Environ.* 266, 118707.
- Szép, R., Mateescu, E., Nită, I.-A., Birsan, M.-V., Bodor, Z., Keresztesi, Á., 2018. Effects of the Eastern Carpathians on atmospheric circulations and precipitation chemistry from 2006 to 2016 at four monitoring stations (Eastern Carpathians, Romania). *Atmos. Res.* 214, 311–328.
- Wang, H., Han, G., 2011. Chemical composition of rainwater and anthropogenic influences in Chengdu, Southwest China. *Atmos. Res.* 99, 190–196.
- Wang, Z.-J., Yue, F.-J., Wang, Y.-C., Qin, C.-Q., Ding, H., Xue, L.-L., Li, S.-L., 2022. The effect of heavy rainfall events on nitrogen patterns in agricultural surface and underground streams and the implications for karst water quality protection. *Agric. Water Manag.* 266, 107600.
- Wu, Q., Han, G., 2015. Sulfur isotope and chemical composition of the rainwater at the Three Gorges Reservoir. *Atmos. Res.* 155, 130–140.
- Wu, Q., Han, G., 2018. 813CDIC tracing of dissolved inorganic carbon sources at Three Gorges Reservoir, China. *Water science and technology. a journal of the International Association on Water Pollution Research* 77, 555–564.
- Wu, Q., Han, G., Tao, F., Tang, Y., 2012. Chemical composition of rainwater in a karstic agricultural area, Southwest China: the impact of urbanization. *Atmos. Res.* 111, 71–78.
- Wu, Y., Xu, Z., Liu, W., Zhao, T., Zhang, X., Jiang, H., Yu, C., Zhou, L., Zhou, X., 2016. Chemical compositions of precipitation at three non-urban sites of Hebei Province, North China: influence of terrestrial sources on ionic composition. *Atmos. Res.* 181, 115–123.
- Xiao, H.-W., Xiao, H.Y., Zhang, Z.y., Wang, Y.-L., Long, A.-m., Liu, C.Q., 2016. Chemical characteristics and source apportionment of atmospheric precipitation in Yongxing Island. *China Environ. Sci.* 36, 3237–3244 (in Chinese).
- Xu, W., Wen, Z., Shang, B., Dore, A.J., Tang, A., Xia, X., Zheng, A., Han, M., Zhang, L., Zhao, Y., Zhang, G., Feng, Z., Liu, X., Zhang, F., 2020. Precipitation chemistry and atmospheric nitrogen deposition at a rural site in Beijing, China. *Atmos. Environ.* 223, 117253.
- Xu, Z., Han, G., 2009. Chemical and strontium isotope characterization of rainwater in Beijing, China. *Atmos. Environ.* 43, 1954–1961.
- Xu, Z., Li, Y., Tang, Y., Han, G., 2009. Chemical and strontium isotope characterization of rainwater at an urban site in Loess Plateau, Northwest China. *Atmos. Res.* 94, 481–490.
- Xu, Z., Tang, Y., Ji, J., 2012. Chemical and strontium isotope characterization of rainwater in Beijing during the 2008 Olympic year. *Atmos. Res.* 107, 115–125.
- Xu, Z., Wu, Y., Liu, W.-J., Liang, C.-S., Ji, J., Zhao, T., Zhang, X., 2015. Chemical composition of rainwater and the acid neutralizing effect at Beijing and Chizhou city, China. *Atmos. Res.* 164–165, 278–285.
- Yang, B., Wang, Y., Nan, S., 2021a. Joint influence of anomalous medium- and small-scale circulations on short-term heavy rainfall events over Beijing. *Int. J. Climatol.* 41, 1002–1023.
- Yang, F., Tan, J., Shi, Z.B., Cai, Y., He, K., Ma, Y., Duan, F., Okuda, T., Tanaka, S., Chen, G., 2012. Five-year record of atmospheric precipitation chemistry in urban Beijing, China. *Atmos. Chem. Phys.* 12, 2025–2035.
- Yang, L., Ni, G., Tian, F., Niyogi, D., 2021b. Urbanization exacerbated rainfall over European suburbs under a warming climate. *Geophys. Res. Lett.* 48, e2021GL095987.
- Yang, L., Smith, J., Niyogi, D., 2019. Urban impacts on extreme monsoon rainfall and flooding in complex terrain. *Geophys. Res. Lett.* 46, 5918–5927.
- Zeng, J., Han, G., 2021. Rainwater chemistry observation in a karst city: variations, influence factors, sources and potential environmental effects. *PeerJ* 9, e11167.
- Zeng, J., Han, G., Wu, Q., Tang, Y., 2020a. Effects of agricultural alkaline substances on reducing the rainwater acidification: insight from chemical compositions and calcium isotopes in a karst forests area. *Agric. Ecosyst. Environ.* 290, 106782.
- Zeng, J., Yue, F.-J., Li, S.-L., Wang, Z.-J., Qin, C.-Q., Wu, Q.-X., Xu, S., 2020b. Agriculture driven nitrogen wet deposition in a karst catchment in southwest China. *Agric. Ecosyst. Environ.* 294, 106883.
- Zeng, J., Yue, F.-J., Li, S.-L., Wang, Z.-J., Wu, Q., Qin, C.-Q., Yan, Z.-L., 2020c. Determining rainwater chemistry to reveal alkaline rain trend in Southwest China: evidence from a frequent-rainy karst area with extensive agricultural production. *Environ. Pollut.* 266, 115166.
- Zeng, J., Yue, F.-J., Wang, Z.-J., Wu, Q., Qin, C.-Q., Li, S.-L., 2019. Quantifying depression trapping effect on rainwater chemical composition during the rainy season in karst agricultural area, southwestern China. *Atmos. Environ.* 218, 116998.
- Zeng, J., Yue, F.-J., Xiao, M., Wang, Z.-J., Wu, Q., Qin, C.-Q., 2020d. Dissolved organic carbon in rainwater from a karst agricultural area of Southwest China: variations, sources, and wet deposition fluxes. *Atmos. Res.* 245, 105140.
- Zhang, D.D., Jim, C.Y., Peart, M.R., Shi, C., 2003. Rapid changes of precipitation pH in Qinghai Province, the northeastern Tibetan Plateau. *Sci. Total Environ.* 305, 241–248.
- Zhang, M., Wang, S., Wu, F., Yuan, X., Zhang, Y., 2007. Chemical compositions of wet precipitation and anthropogenic influences at a developing urban site in southeastern China. *Atmos. Res.* 84, 311–322.
- Zhang, S., Ma, Z., Li, Z., Zhang, P., Liu, Q., Nan, Y., Zhang, J., Hu, S., Feng, Y., Zhao, H., 2021a. Using CYGNSS data to map flood inundation during the 2021 extreme precipitation in henan province, China. *Rem. Sens.* 13, 5181.
- Zhang, Y., Gao, Y., Guo, L., Zhang, M., 2021b. Numerical analysis of aerosol direct and indirect effects on an extreme rainfall event over Beijing in July 2016. *Atmos. Res.* 264, 105871.
- Zhang, Y., Lee, X., Cao, F., Huang, D., 2011. Seasonal variation and sources of low molecular weight organic acids in precipitation in the rural area of Anshun. *Chin. Sci. Bull.* 56, 1005–1010.
- Zhong, S.-x., Zhuang, Y., Hu, S., Chen, Z.-t., Ding, W.-y., Feng, Y.-r., Deng, T., Liu, X.-t., Zhang, Y.-x., Xu, D.-s., Dai, G.-f., Meng, W.-g., 2021. Verification and assessment of

real-time forecasts of two extreme heavy rain events in Zhengzhou by operational NWP models. *J. Trop. Meteorol.* 27, 406.

Zhou, X., Bai, Z., Yang, Y., 2017. Linking trends in urban extreme rainfall to urban flooding in China. *Int. J. Climatol.* 37, 4586–4593.

Zhou, X., Xu, Z., Liu, W., Wu, Y., Zhao, T., Jiang, H., Zhang, X., Zhang, J., Zhou, L., Wang, Y., 2019. Chemical composition of precipitation in Shenzhen, a coastal megacity in South China: influence of urbanization and anthropogenic activities on acidity and ionic composition. *Sci. Total Environ.* 662, 218–226.